

A quadratic boost converter derived multi output converter for electric vehicles application

Original Scientific Paper

I. S. Sree Devi

Noorul Islam Centre for Higher Education
Kumarakovil, TamilNadu, India
issredevieeee@gmail.com

D. M. Mary Synthia Regis Prabha

Noorul Islam Centre for Higher Education
Kumarakovil, TamilNadu, India
regisprabha@gmail.com

Abstract – A novel Solar Photo Voltaic Powered dual output DC to DC converter with the Quadratic Boost Converter as the core element, typically for Electrical Vehicle applications has been proposed and validated in this work. The proposed system harvests the solar power and charges a 12 V battery, supplies power to a 12 V load, using the buck feature of the proposed converter. A second channel of 48 V output is derived using the boost channel and the 48 V output is meant for driving the traction motor as well as any other load that requires a regulated 48 V. The proposed converter can operate in three different modes. For the purpose of voltage regulation at the 48 V and 12 V output channels and for the Maximum Power Point Tracking, applicable to the Solar Photo Voltaic source, individual Sliding Mode Controllers are used. The proposed idea has been validated using simulations in the MATLAB SIMULINK environment and an experimental prototype.

Keywords: harvesting solar photo voltaic energy, quadratic boost derived converter, multiple output dc to dc converters, sliding mode controllers, dual output converter

1. INTRODUCTION

Electrically powered vehicles of all ranges of power ratings are encouraged globally. The EV sector includes all transportation systems from the E bike to the electrically actuated city buses and so on. EVs are also included in the fleet of garbage management systems in big and smart cities as well as industrial transportation systems. The electrically actuated two wheeler bikes, which can carry two persons, use BLDC motors which require 48 V DC. The three wheeler type garbage collecting EVs used in major cities use the BLDC motor or the DC motor as the drive element and it is rated at 48 V. In the case of three wheeler type garbage collection and transportation system the main source of power is the Solar Photo Voltaic (SPV) panels mounted on the top and sides of the body of the vehicles. There is a standard battery backup of voltage rating 12 V and of nickel ion or lead acid type. These vehicles also have charging facility using which the battery can be charged directly from the utility AC source when the vehicle is parked in the standby condition. [1 – 4] Essentially these systems have three entities namely the SPV source, the battery and the BLDC motor. Although the SPV panels have a certain rated voltage and cur-

rent, because of the changes in the solar irradiance and temperature the terminal voltage of the SPV panel will have to be maintained at the optimal voltage for enabling maximum power point tracking system. Thus the SPV panel becomes a variable voltage, variable power output source. This variable DC voltage source is used by a DC to DC converter to charge the battery that is nominally rated at 12 V. The required operating voltage of the BLDC motor is 48 V. The BLDC motor may use either a voltage controlled speed control mechanism or a current controlled PWM scheme for the speed control. Thus three different voltages are involved in the system. Therefore a DC to DC power conversion system converter that can deliver the required voltage to the 12 V battery from the SPV panel or from the utility source and the required 48 V to the BLDC motor drive system is required.

In [5] the authors have developed an off line battery charging system and in [6] the authors have developed an electric vehicle for a typical school bus application. Since an automobile, especially an electrical vehicle uses a number of electrical systems which require different voltage levels, DC to DC converters with multi input multi output features are required. The main drive

system may use a higher DC voltage while the control systems, lights, AC, video monitors, navigational systems etc. may require diversified DC voltage levels.

Since many of the electrical vehicles use drives which require at least 48 V, when the backup source is a 12 V DC battery, high voltage gain DC to DC converters are required. In [7] a switched reluctance motor based drive system has been developed and the system uses a high voltage gain DC to DC converter. In [8 -9] the authors have adopted a hybrid DC to DC conversion system that combines the topologies of the Quadratic Boost converter and the Cuk or with the SEPIC converter. The Quadratic Boost Converter (QBC) has also evolved as a high voltage gain DC to DC converter. The authors in [10] have developed and validated the concept of QBC.

Considering the non linearity and the variable structure nature of the power electronic converters the Sliding Mode Controller (SMC) is encouraged. Several researchers have used the SMC for parameter regulation as well for maximum power point tracking of the renewable resources [11 - 13].

A proliferation of multiport DC to DC conversion systems are available and the authors in [14] and [15] have presented multiport DC to DC conversion systems using hybrid energy sources.

The authors in [16] have presented a bidirectional power conversion scheme that has proved to be comparatively more efficient. The authors in [17] have developed a non-isolated high step- up DC-DC converter featuring soft switching for hybrid energy systems. Quadratic boost converter is discussed in detail in [18]-[21]. A combination of an isolated and a non isolated multiple output topology was proposed and validated by the authors in [22]. A multi input SPV energy harvesting system with a DC to DC converter has been demonstrated in [23]. The authors in [23] have also included an MPPT feature in this work. An interesting power flow control scheme for a dual input interleaved converter with buck and boost features has been demonstrated by the authors in [24]. An AC link converter topology for a solar powered inverter was proposed and validated by the authors in [25]. The high frequency resonant AC link enables zero voltage switching leading to reduced switching losses and increased power conversion efficiency. The authors in [26] have proposed and validated a battery charging system for the nanogrid using a set of multiple sources governed by a common control. Further in [27] a two stage bidirectional AC/DC converter that uses a renewable energy source governed by a suitable control loop design has been proposed and validated. In a similar development, a bidirectional micro inverter with a dual active bridge scheme with ultra capacitor based energy storage system powered by modular SPV source was proposed and validated in [28]. In the article [29] a novel bidirectional converter for the support of a residential DC distribution system with a grid interface for the SPV source has been presented. The same authors

as in [29] have made another contribution [30] wherein a novel grid interface with a two stage power conversion scheme has been promoted.

To this end, a review of the literature suggests that a solar power harvesting system with high voltage gain, bidirectional power transaction, energy storage and backup feature and multiport outputs are an absolute necessity in the modern electric vehicle industry. In this work a novel Quadratic Boost Derived Multi Output Converter(QBDMOC) is designed and is used to deliver a 48 V boost output and 12 V stepdown output. . The control scheme adopted uses the Sliding Mode Controller (SMC) and this ensures the harvest of maximum power from the solar PV system for the given solar irradiation.

The paper is arranged as follows. Next to this brief introduction, in section 2, an outline of the proposed system is presented. The state space averaged model of the QBC is presented in section 3. The realization of the proposed system in MATLAB SIMULINK environment is given in section 4. The details of the experimental verification and the results obtained in simulations and in the experimental verifications have been discussed about in section 5. The conclusion and the references section follow.

2. OUTLINE OF THE PROPOSED SYSTEM

The general structure of the proposed system is shown in Fig. 1. It draws power from the SPV source and optionally the utility source can be used. There are two output voltages and they are maintained at 12 V (LV) and 48 V (MV). Fig. 1 shows the configuration in which the 12 V battery, a load for the LV bus and a load for the MV bus are used. Across the MV bus bar, an R or RL load is used or as shown in Fig. 2, typically a BLDC motor can be used. The features of the proposed system are it can generate a 48 V DC supply from a battery or from the SPV source or from the Utility source. Depending upon the availability and the strength of the different sources and the requirement of the load, the different modes are selected. The topology of the core power electronic converter used in the proposed system is similar to a Quadratic Boost Converter.

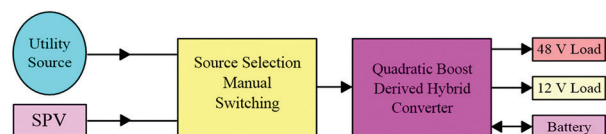


Fig. 1. Proposed dual output DC to DC converter

In addition, the system uses an additional power electronic switch for delivering a stepped down voltage output, typically 12 V for either charging the battery or for delivering power for the 12 V load. With reference to the circuit diagram shown in Fig. 3 there are two individual switches SW_1 and SW_2 and a set of switches grouped as GS. SW_1 can connect or discon-

nect the external source to the converter unit. The switch SW_2 can be used to connect or disconnect the 48 V load denoted as Load 2.

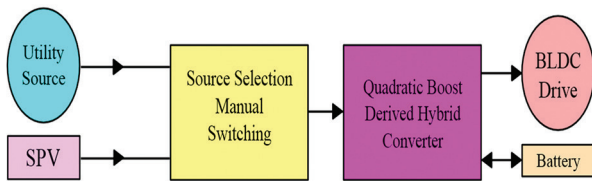


Fig. 2. An Application of the proposed system

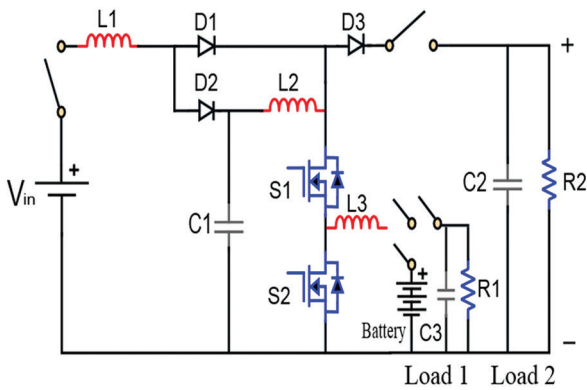


Fig. 3. Schematic of the proposed system

The switch group GS can be used to connect the battery to the rest of the circuit for charge or discharge modes of operation. Using the switch group GS, the low voltage load, denoted as Load1, can be connected or disconnected to the battery or to the converter. Some of the important modes of operation which could be realized using these are,

Mode. 1. The input source voltage is available. (Buck Mode) (SW_1 On; SW_2 Off; GS: Battery connected to converter). In this mode only the battery gets charged.

Mode. 2. The source voltage is not available. (SW_1 Off; SW_2 On; GS: battery connected to converter). The boost converter draws power from the 12 V battery and drives Load 2 with 48 V regulated supply. The battery is now discharging.

Mode. 3. The main input source is available. (Buck and Boost (QBC))

Load 1 and load 2 are operational. The battery can also be charged.

3. THE DETAILS OF THE SUBSYSTEMS

3.1 STATE SPACE ANALYSIS OF THE QUADRATIC BOOST CONVERTER

Since the QBC is the heart of the system the state space analysis of the QBC is developed and considering the steady state condition from the state equation the voltage gain of the QBC is derived. The voltage gain of the GBC and the QBC are shown in equations (1) and (2) respectively

$$V_o = \frac{V_{in}}{(1-D)} \quad (1)$$

$$V_o = \frac{V_{in}}{(1-D)^2} \quad (2)$$

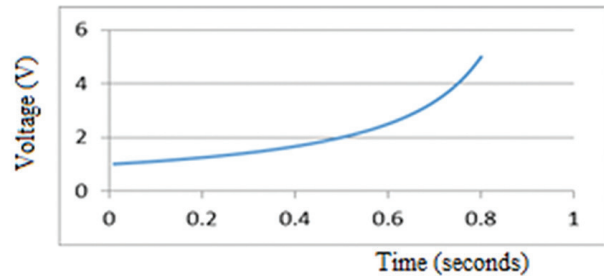


Fig. 4. Voltage gain variation of boost converter

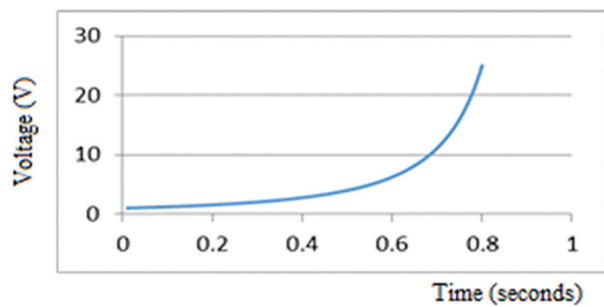


Fig. 5. Voltage gain variation of proposed converter

Fig.4 and Fig. 5 shows the duty cycle D versus voltage gain of the generic boost converter and proposed converter respectively. With reference figures 4 and 5 it can be seen that the voltage gain of the QBC is much higher than that of the GBC.

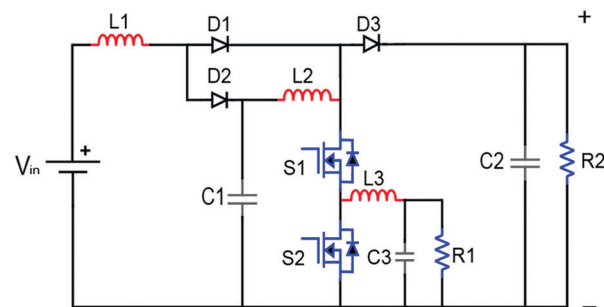


Fig. 6. Topology of the Quadratic boost derived hybrid converter

The topology of the proposed system is given in Fig.6

3.2 THE SOLAR PHOTO VOLTAIC SOURCE

Here, the SPV source is the primary source of power. Six numbers of similar panels are used in parallel. The VI and the VP characteristics of one of the SPV panel are shown in Fig. 7.

With reference to Fig. 7 it is clear that the solar power output will be maximum, for any given solar irradiation, if and only if the terminal voltage of the SPV subsystem is maintained at a specific value while it delivers a spe-

cific current as well. In this work the SMC technique is used for MPPT. The advantage of the SMC technique is that, unlike the perturb and observe algorithm and the incremental conductance algorithm for MPPT, the SMC based MPPT scheme requires only the terminal voltage of the SPV unit need to be monitored.

In MPPT system, as applied to SPV systems, the set or the desired value of the controlled parameter is a dynamic one. Since the power electronic switches can be switched at high frequencies the SMC can track the desired level easily.

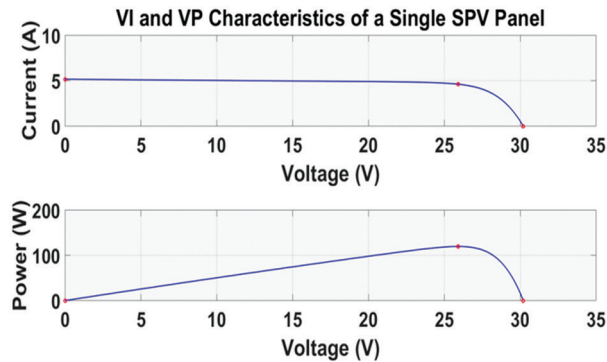


Fig.7. VI and VP characteristics of one of the SPV panels

3.3 SMC AS A MPPT CONTROLLER

The ratio between V_{pmax} and V_{oc} is a constant of the panel, which we denote as G , and the operating terminal voltage of the SPV panel should be adjusted in real time that the constant G is always maintained.

The algorithm for the SMC based MPPT is as follows.

1. Keep the power converter in the OFF state.
2. Measure the Open Circuit Terminal Voltage of the SPV unit. (V_{oc})
3. Turn on the power converter.
4. Measure the Terminal Voltage of the SPV unit (V_{pv}).
5. Is $(V_{pv} / V_{oc}) < G$ (G is the constant and is V_{pmax} / V_{oc}).
6. If yes, turn OFF the power converter and go to step 1.
7. Else keep power converter ON and go to step 4.

3.4 SCHEME OF CONTROL

There are some operational modes selected manually, as given earlier in the outline section. Besides, there are some requirements to be fulfilled automatically by the proposed control systems. The automatic closed loop control schemes have been built to satisfy the following requirements or objectives.

- There must be a provision for MPPT.
- The voltage across Load 2 should be maintained at 48 V

- The load across Load 1 should be maintained at 12 V.

In the proposed system the switch S_1 is primarily meant for buck operation to deliver a 12 V supply across Load1 or charge the 12 V battery. The switch S_2 is primarily meant for the boost operation. There are two control sub systems and they are meant for the buck and the boost converter switches S_1 and S_2 respectively. For the boost converter a fixed duty cycle of 0.6 is used. This will provide a voltage gain of $(1 / (1 - 0.6)^2) = 6.25$. If the source voltage is as low as 10 V the maximum possible output voltage could be 62.5 V. The duty cycle of the buck converter is 0.8 and if the source voltage is as low as 15 V the output voltage could be 12 V.

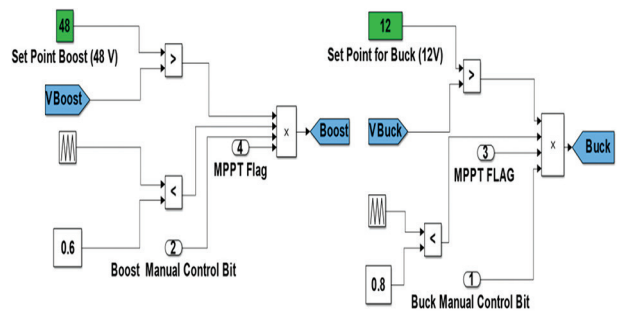


Fig. 8. Control subsystems.

Fig. 8 shows the control scheme adopted as realized in the MATLAB SIMULINK environment.

3.5. INTERLOCKING CONTROL SCHEME

In the proposed system, for the QBC based boost mode of operation the switches S_1 and S_2 should be operational. It is possible that the voltage across load 1 reaches the 12 V level earlier than the instant the voltage across Load 2 reaches 48 V. In this scenario according to the control scheme logic switch S_1 will be turned off. This will stop the functioning of the QBC and the voltage across Load 2 cannot be built up to the required 48 V level. According to the control system, only S_2 will be getting the required switching pulses. This will enable the capacitor across Load 1 to act as a source and the S_2 along with the inductor L_3 and the diode of S_1 will form a generic boost converter trying to pump power to the 48 V load. This causes the voltage across the Load1 to become little less than 12 V level bringing again S_1 also to be functional and the QBC comes back to form. This process continues until the voltage across Load1 and Load2 reach 12 V and 48 V level respectively.

3.6. DIFFERENT MODES OF OPERATION AND POWER BALANCE

Mode 1: The different modes of operations and the corresponding circuit arrangements are shown in Fig.9 to 11. Fig. 9 shows the battery charging mode or the 12 V load driving mode. In this mode the 48 V load is turned off. The power control switch S_1 is operational in

the buck mode. The diode inside S_2 is used as the free-wheeling diode. The control system regulates the load side voltage at 12 V. In the same mode of operation, if an SPV is used for the source and a battery is used for the load then the battery is charged satisfying the MPPT requirement.

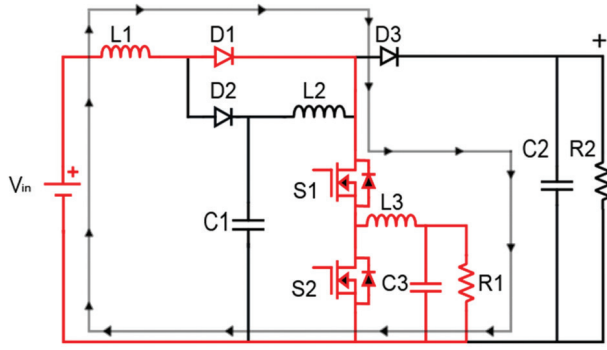


Fig. 9. Buck mode of operation

Fig. 10 gives the circuit arrangement of the buck and the boost mode of operation. The S_1 and S_2 are operational and the load side voltages of 12 V and 48 V are regulated across the respective loads.

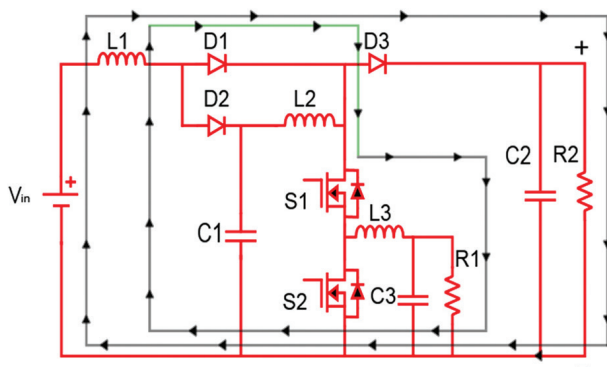


Fig. 10. Buck and boost modes of operations

Fig. 11 shows the scenario when the external source is absent and the 48 V load is operational. The battery supplies the required power to the 48 V load. The circuit obeys the voltage gain equation of the generic boost converter.

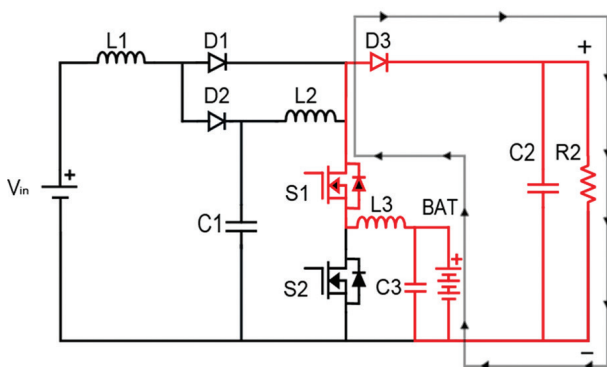


Fig. 11. Boost mode powered from the battery

4. REALIZATIONS IN MATLAB SIMULINK AND THE RESULTS

The proposed system has been realized in MATLAB SIMULINK and the various subsystems are presented in Fig.12 to 14. Fig. 12 shows the SPV and the MPPT subsystems. Fig. 13 shows the internal structure of the SMC based MPPT scheme. The constant 0.857 is the constant of the solar panel used and it has been derived using equation (3)

$$G = \frac{V_{pmax}}{V_{oc}} = \frac{25.9}{30.2} = 0.857 \quad (3)$$

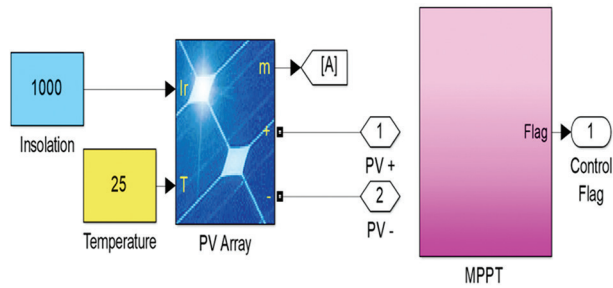


Fig. 12. SPV Subsystem

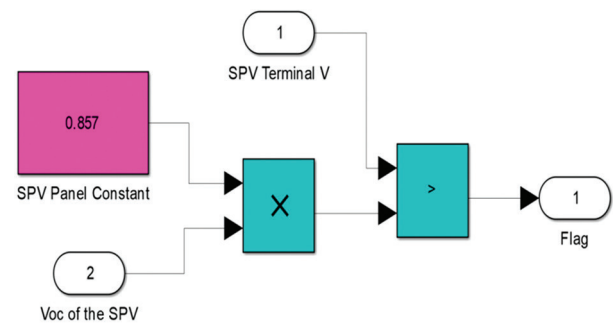


Fig. 13. MPPT subsystem

Fig. 13 shows the MPPT subsystem. To start with, the control system monitors the open circuit voltage of the SPV and calculates the required voltage to be maintained across the SPV subsystem. Then the power converter is actuated until the terminal volts falls down to the V_{pmax} level from the V_{oc} level. Once the terminal voltage across the SPV falls just below the V_{pmax} level the converter is switched off. The SPV voltage now rises back to the same V_{oc} level or a new V_{oc} level depending upon the current solar irradiance. The V_{oc} is noted down, the new V_{pmax} is estimated and then the converter is again turned on. The process continues and the required voltage across the SPV panel is thus maintained with a mild chattering and the maximum power harvest is achieved.

Fig. 14 shows the implementation of the proposed system in the MATLAB SIMULINK environment. The two MOSFETs S_1 and S_2 get the required switching pulses from the control system discussed in the earlier section and shown in Fig. 8. The results of the simulations have been recorded for different modes of operation and are presented herein.

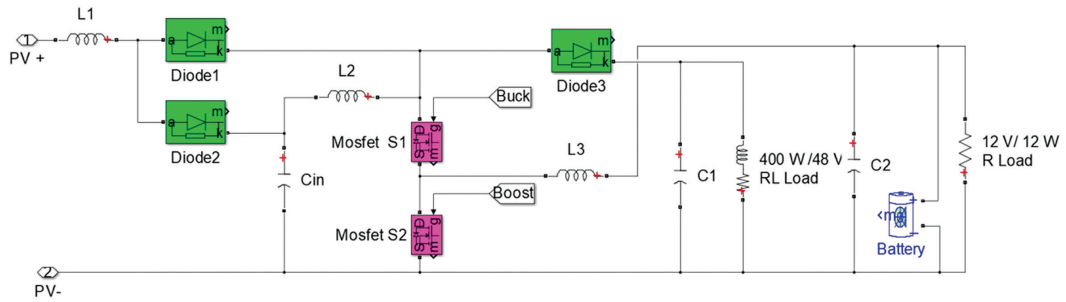


Fig. 14. MATLAB SIMULINK realization of the proposed system

4.1 MODE 1 OPERATION: BATTERY CHARGING FROM EXTERNAL SOURCE

In this mode of operation the battery is charged from the external source. The active part of the circuit is highlighted and is shown in Fig. 9. As a result of a solar irradiance of 1000 W/m^2 , the battery is charged. The related waveforms are shown in Fig. 15 to 21. Fig. 15 shows the solar irradiance of 1000 W/m^2 . The corresponding terminal voltage across the SPV panel is shown in Fig. 16. The terminal voltage across the SPV panel which is nearly 25 V is buck converted to charge the 12 V battery and the battery gets charged with charging current shown in Fig. 18. As a result the State Of Charge of the battery gets increased and is shown in Fig. 19. The voltage across the battery is nearly 12.5 V and is as shown in Fig. 20.

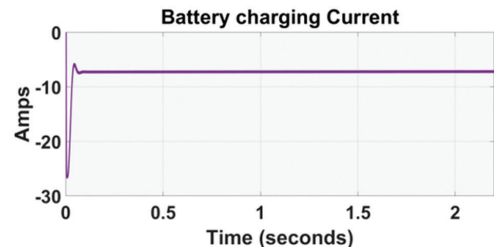


Fig. 18. Battery Charging current

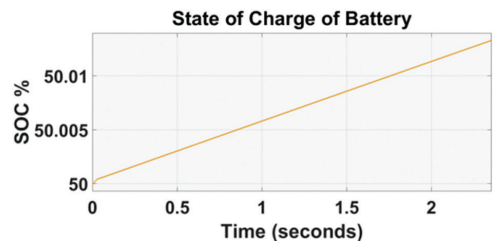


Fig.19. Rise of SOC while charging

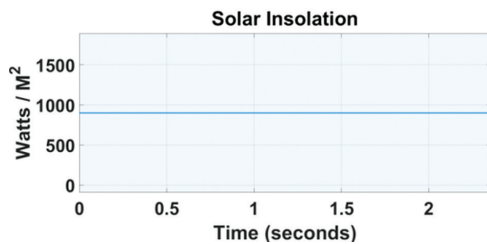


Fig. 15. Solar irradiance of 1000 W/m^2 .

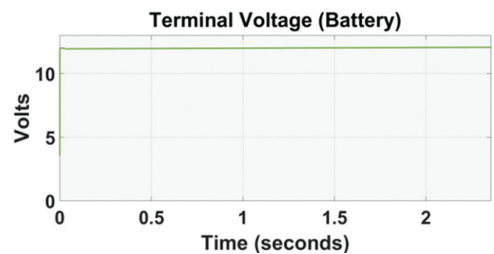


Fig. 20. Battery charging current

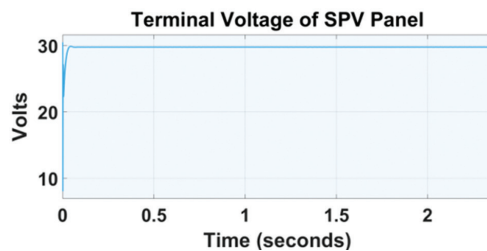


Fig. 16. Terminal voltage across the SPV

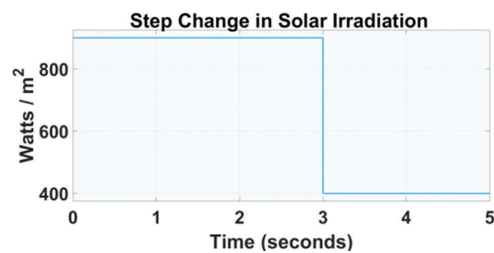


Fig. 21. Step change in solar irradiance

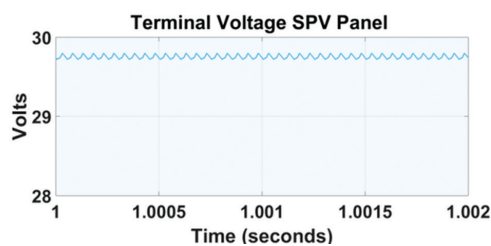


Fig. 17. Ripple in the SPV terminal voltage

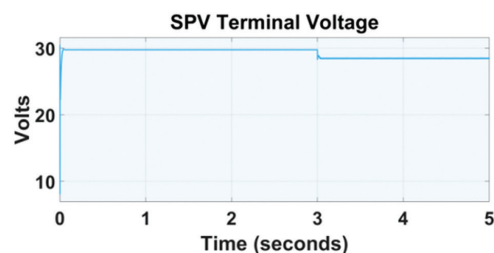


Fig. 22. SPV terminal voltage

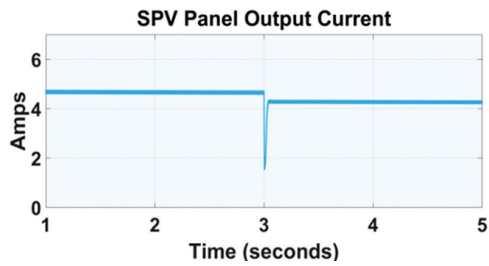


Fig. 23. SPV panel output current

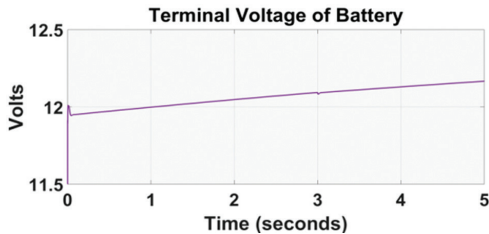


Fig. 24. Rise of Battery voltage

Fig. 21 shows the case of a step change in the solar irradiance from 900W/m^2 to 400W/m^2 . All the related waveforms have been recorded and the important waveforms are shown in Fig. 21 to 24. The change in solar irradiance occurs at time instant 3 sec. and correspondingly the other waveforms reflect. It is observed that there is negligible impact on the loads when there is a step change in input. The transient response of the SPV reflected in terms of the SPV voltage and the SPV output current have been recorded and are as shown in figures 22 and 23. The fall in the solar irradiance results in a fall of the terminal voltage across the SPV terminals and the sudden dip in the SPV current at 3 seconds while the solar irradiance suddenly falls.

4.2 MODE 2: DELIVERING POWER TO THE 48 V LOAD

In this mode of operation corresponds to the circuit arrangement shown in Fig. 11. The external source is not used. The battery supplies the required power for the 48 V load. The SOC of the battery falls with time. The terminal voltage across the load and the battery discharge current are shown in Fig.25- 27. The discharge current from the battery is positive.

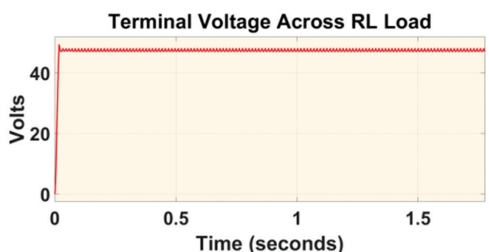


Fig. 25. Terminal voltage across Load2

The proposed system is intended to deliver an output voltage of 48 V in the high voltage output channel. The transient response of the output voltage, when a command is given at time instant 0 is given, is shown in fig-

ure 25. the rise time of the output voltage was observed to be 0.02 second. The peak overshoot was observed to be 49.5 V and the steady state error was found to be 0.05 as the output voltage was regulated at 48.05 V.

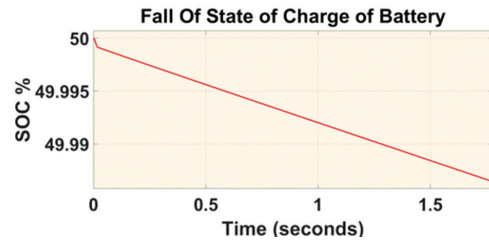


Fig. 26. SOC of battery

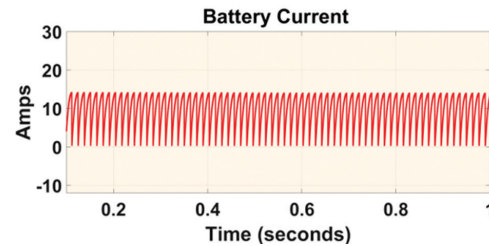


Fig. 27. Battery current (Discharging)

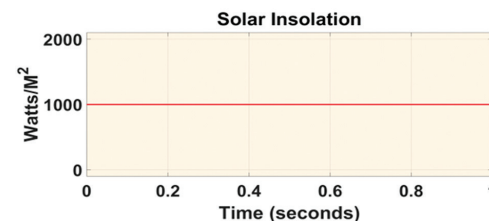


Fig. 28. Solar irradiation

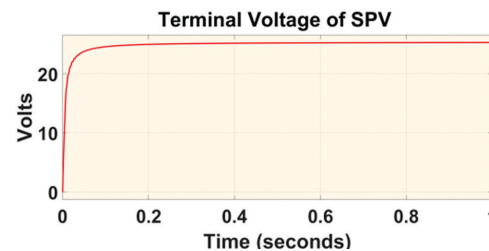


Fig. 29. Terminal voltage of SPV

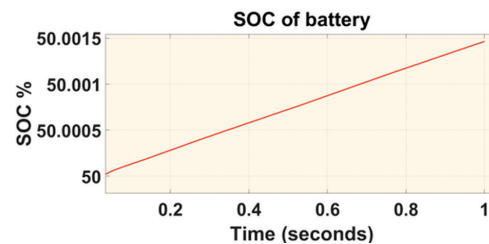


Fig. 30. SOC of the battery

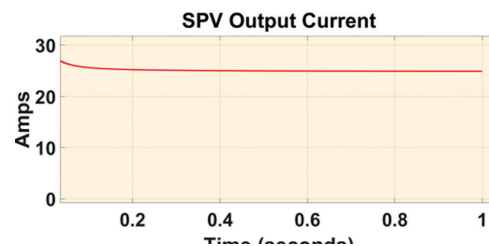


Fig. 31. Output current of SPV

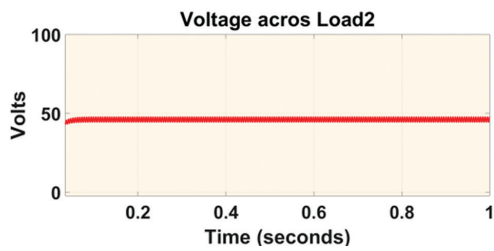


Fig. 32. Voltage across Load 2

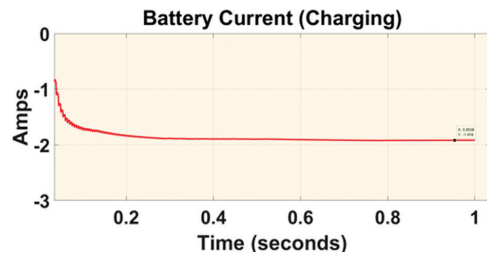


Fig. 33. Battery charging current

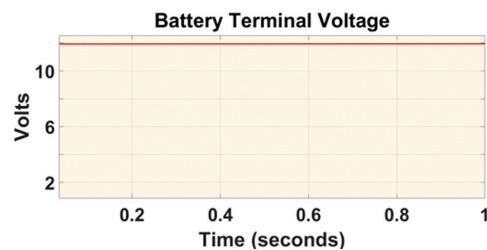


Fig. 34. Battery terminal voltage

4.3 MODE 3: BUCK AND BOOST MODE OF OPERATION

In this mode both the loads are operational. Fig. 29 to 34 correspond to the case of the external source delivering power to the 48 V load as well the battery is charged. The circuit arrangement shown in fig. 10 corresponds to this mode of operation. With a solar irradiance of 1000 W/m^2 , the maximum power harvested is shared among the loads without any wastage. Table 1 & 2 gives the specifications of the components used and the values of some important parameters.

Table 1. Nominal parameters and specifications of components

Parameter / Component	Specification
Power Electronic Switches	MOSFET
Inductor L_1	500 μH
Inductor L_2	500 μH
Capacitor C_1	2200 μF
Capacitor C_2	2200 μF
Nominal Input voltage	12 to 19 V
Buck output for Battery	12 V
Boost output for Load	48 V
Nominal load @ 48 V	500 W
Nominal load @ 12 V	300W

Table 2. Specifications of the SPV Panel and the battery

SPV panel	Specification
Max. Power rating of panel	120 W
Open Circuit Voltage	30.2 V
Short Circuit Current	5.15 A
Voltage at P_{max}	25.9 V
Current at P_{max}	4.63 A
Number of panels in series	1
Number of panels in Parallel	6
Storage Battery	
Type	Lead Acid
Nominal Terminal Voltage	12 V
Capacity	35 Ah

5. HARDWARE DESCRIPTION

The major components of the setup include the SPV panel, the battery the proposed converter system and the resistive loads for the 12 V and 48 V channels of loads. The SPV system can deliver a maximum power output of 125 W at a solar irradiance of 1000 W/m^2 and 25°C . The battery is rated 12 V and 35 Ah. An R load of $50 \Omega / 50\text{W}$ is powered by the system. The excess energy harvested is stored in the battery. When the SPV is not available the battery supplies the load. The system therefore has a buck mode of operation and a boost mode of operation happening simultaneously. The buck converter charges the battery while the boost converter supplies the required 48 V to the load. The proposed system uses an SMC for the maintenance of the 48 V across the load. The switching pulses produced by the SMC drives the MOSFET through the opto coupler.



Fig. 35. Photograph of the proposed system

The algorithm can be implemented in the PIC Micro controller. The PIC Micro Controller 16F877 A has built in ADCs using which the terminal voltage of the panel and any other analog quantities to be considered could be read into. In the case of the quadratic boost derived hybrid converter topology, it is necessary that the power electronic switch be applied with a square pulse of a

fixed duty cycle that can produce the required output voltage and MPPT.

The power electronic switches used in the buck and the boost sections are of type IRF 540 and they are protected with snubber circuits. The hardware prototype uses an optical isolation between the control circuit and the power circuit. The control circuit consists of the micro controller. The power circuit consists of the main source of power, the load, the battery and the power electronic switches and the storage elements like L and C which form the topology.

The specifications of the system under consideration are shown in table 3.

Table 3. Specifications of the Proposed System

Parameters	Specifications
Capacity of SPV Source	125 W
Open circuit voltage	22.2 V
Short Circuit Current	7.75 A.
Voltage at Pmax	17.2 V
Current at Pmax	7.25 A.
The MOSFETs	IRF 540
Opto Coupler	MCT2E

The wave forms of the various currents and the voltages have been recorded and are presented herein. Fig. 35 shows the terminal voltage of the SPV panel when there is no load on the SPV panel. It has been observed that for the given climatic conditions the open circuit voltage of the SPV panel is 9.1 V. With the battery as the load, for the available solar irradiance the battery gets charged. The switching pulses applied to the buck converter switch SW1 is shown in Fig. 37. The charging current is shown in Fig. 38.

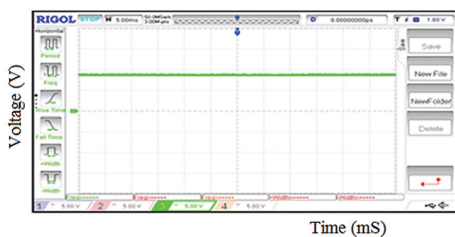


Fig. 36. SPV panel terminal Voltage with No load on the SPV (Low Solar Irradiance; $V_{pv} = 9V$)

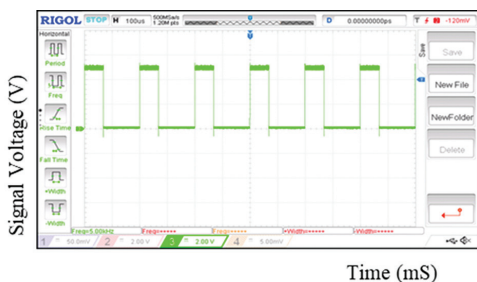


Fig. 37. Switching pulses applied to the buck converter.

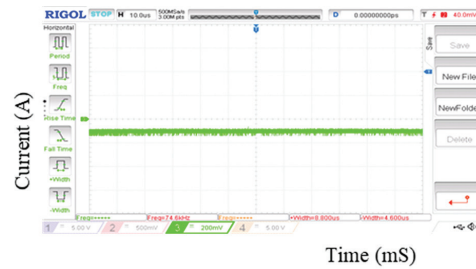


Fig. 38. Battery while charging. (Scenario 1)

When the quadratic boost converter is in action the two inductors L_1 and L_2 play important role in boosting up the voltage from the SPV panel which is as low as 15.2 V as shown in Fig. 39, to a load side voltage of 48 V. Fig.41 shows the load side voltage of 48 V when the system is fed directly from the SPV panel, without the support of the battery. In this mode of operation switches S_1 and S_2 should work and the voltage across the series combination of S_1 and S_2 is shown 40.

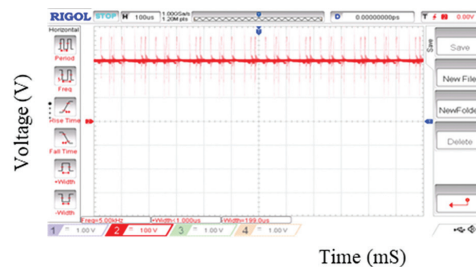


Fig. 39. SPV terminal voltage

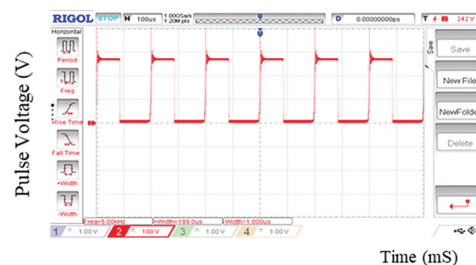


Fig. 40. Voltage across the switch S1 and S2

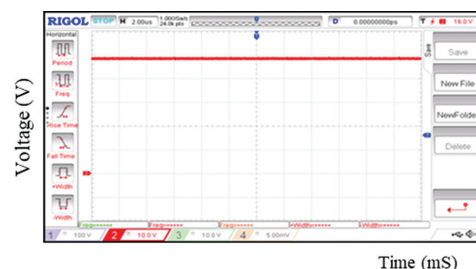


Fig. 41. Voltage across the load = 48 V

When the SPV source is not available, the battery is the only source and it gets discharged while supplying power to the 48 V load. In this mode of operation, the generic boost converter operation takes place with L_3 as the boost inductor and SW_2 as the power control switch. The inductor current L_3 current has a continu-

ous component and a pulsating component. The inductor L_3 current is the input current now, and it is the battery discharge current also as shown in Fig. 42.

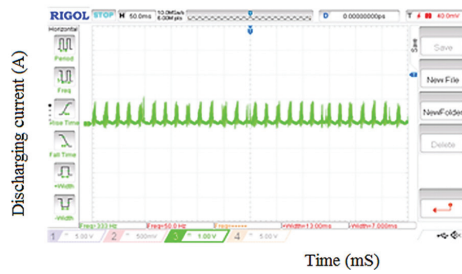


Fig. 42. Battery discharging while no SPV (Scenario 2)

The proposed system can be operated in standby mode also when the SPV power is just used for charging the battery. During this period the loads will not be operational. The power electronic switch S_1 alone works and the internal diode in S_2 acts as the free-wheeling diode. The buck action charges the battery and the battery terminal voltage rises. The battery terminal voltage is as shown in Fig. 43.

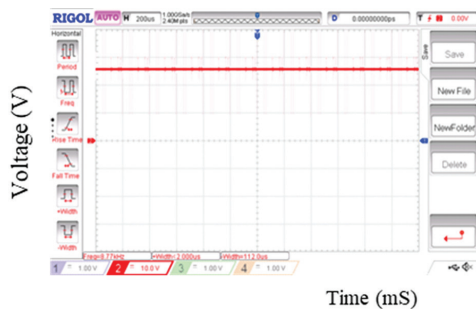


Fig. 43. Voltage across the battery while charging

The control system meant for regulating the output voltage for load 2 at 48 V can be used to regulate any desired load side voltage by just changing the set point. A typical case of regulating the voltage across load 2 at 30 V is shown in Fig. 44.

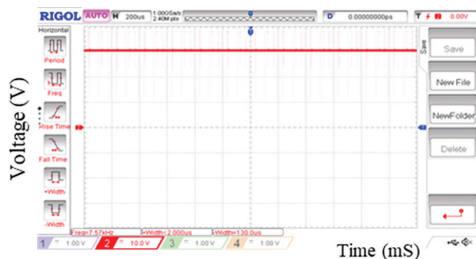


Fig. 44. Voltage across the load when the set value is 30 V

Different scenarios are shown in table 4.

With reference to the tables showing the different scenarios it is clear that when the SPV power is available and if it is more than the demand of the load the

excess power available is routed to the battery through the buck converter. The battery gets charged. It was observed that, for the case when the SPV power generated is 43 W with a terminal voltage of the SPV panel is 14.7 V the SPV current is 2.96 A. Out of this power, the battery is being charged with a terminal voltage across the battery being 12.72 V and the charging current is 3.27A and the total power harvested is routed to the battery.

Table 4. Scenario 1: SPV available Load 48 W Connected.

Source	Power	Voltage	Current
SPV	116 W	19.2 V	6.04 A
Battery	50 W	12.2 V	4.03 A (Charging)
Load2	48 W	48 V	1 A
Load 1	12.4 W	12.2 V	1.016 A
Efficiency	95.19%		

Table 5. Scenario 2: No SPV Source but Load Connected

Source	Power	Voltage	Current
SPV	0 W	0 V	0 A
Battery	65.8 W	11.9 V	5.53 A (Discharging)
Load2	48 W	48 V	1 A
Load 1	11.8 W	11.9 V	0.991 A
Efficiency	90.87%		

Table 6. Scenario 3 SPV Source Available but No Load

Source	Power	Voltage	Current
SPV	43 W	14.7 V	2.96 A
Battery	40 W	12.72 V	3.27 A (Charging)
Load2	0 W	48 V	0 A
Load 1	0 W	0 V	0 A
Efficiency	95.5%		

With reference to the tables showing the different scenarios it is clear that when the SPV power is available and if it is more than the demand of the load the excess power available is routed to the battery through the buck converter.

The battery gets charged. It was observed that, for the case when the SPV power generated is 43 W with a terminal voltage of the SPV panel is 14.7 V the SPV current is 2.96 A. Out of this power, the battery is being charged with a terminal voltage across the battery being 12.72 V and the charging current is 3.27A and the total power harvested is routed to the battery.

6. CONCLUSION

A novel dual output DC to DC converter built around a QBC has been presented. The mathematical modeling using the State Space averaging technique has been presented. The open circuit behavior of the proposed QBDMOC has been studied. The proposed converter has been powered by an SPV source. SMC scheme has been used for the MPPT as well as for regulating the output voltages. The different modes of operations have been simulated and the proposed idea has been validated. An experimental prototype has also been developed and the proposed idea has been verified successfully. It has been observed that both in the simulation and in the experimental verification the proposed topology exhibited the expected functionality by delivering a regulated 48 V output at the high voltage channel and a regulated 12 V output at the low voltage channel. The MPPT scheme using the SMC has proved to track the changes in the solar irradiance and helps to harvest the maximum power at all solar irradiances. Efficiency can be improved by designing advanced controller. Novel converter can be designed by interfacing n number of converters to get n number of multilevel outputs.

7. REFERENCES

- [1] J. Malan, M. J. Kamper, "Performance of a hybrid electric vehicle using reluctance synchronous machine technology", *IEEE Transactions on Industry Applications*, Vol. 37, No. 5, 2001, pp. 1319-1324.
- [2] F. Musavi, W. Eberle, W. G. Dunford, "A high-performance single-phase AC-DC power factor corrected boost converter for plug in hybrid electric vehicle battery chargers", *Proceedings of the IEEE Energy Conversion Congress and Exposition*, Atlanta, GA, USA, 12-16 September 2010, pp. 3588-3595.
- [3] Z. Chen, Z. Nie, Y. Fu, C. C. Mi, "A bidirectional power converter for battery of plug-in hybrid electric vehicles", *Proceedings of the IECON 36th Annual Conference on IEEE Industrial Electronics Society*, Glendale, AZ, USA, 7-10 November 2010, pp. 3049-3053.
- [4] S. Ketsingsoi, Y. Kumsuwan, "An Off-line Battery Charger Based on Buck-Boost Power Factor Correction Converter for Plug-in Electric Vehicles", *Energy Procedia*, vol. 56, 2014, pp. 659-666.
- [5] P. H. Kydd, C. A. Martin, K. J. Komara, P. Delgoshaei, D. Riley, "Vehicle-Solar-Grid Integration II: Results in Simulated School Bus Operation", *EEE Power and Energy Technology Systems Journal*, Vol. 3, No. 4, 2016, pp. 198-205.
- [6] M. A. Mingyao, Z. Chang, Y. hu, C. Gan, W. Cao, "An Integrated Switched Reluctance Motor Drive Topology with Voltage-Boosting and On-Board Charging Capabilities for Plug-In Hybrid Electric Vehicles (PHEVs)", *IEEE Access*, Vol. 6, 2017, pp. 1550-1560.
- [7] V. Fernao Pires, A. Cordeiro, D. Foito, J. F. Silva, "High step-up DC-DC converter for fuel cell vehicles based on merged quadratic boost-cuk", *IEEE Transactions on Vehicular Technology*, Vol. 68, No. 8, 2019, pp. 7521-7530.
- [8] S. Natchimuthu, M. Chinnusamy, A. P. Mark, "Experimental Investigation of PV Based Modified SEPIC Converter Fed Hybrid Electric Vehicle (PV-HEV)", *International Journal of Circuit Theory and Applications*, Vol. 48, No. 6, 2020, pp.1-17.
- [9] D. S. Wijeratne, G. Moschopoulos, "Quadratic power conversion for power electronics: principles and circuits", *IEEE Transactions on Circuits and Systems I: Regular Papers*, Vol. 59, No. 2, 2011, pp. 426-438.
- [10] S. H. Chincholkar, C. Y. Chan, "Design of fixed-frequency pulsewidth-modulation-based sliding-mode controllers for the quadratic boost converter", *IEEE Transactions on Circuits and Systems II: Express Briefs*, Vol. 64, No. 1, 2019, pp. 51-55.
- [11] S. W. Lee, H. L. Do, "Quadratic Boost DC-DC Converter with High Voltage Gain and Reduced Voltage Stresses", *IEEE Transactions on Power Electronics*, Vol. 34, No.3, 2019, pp. 1-7.
- [12] G. Li, X. Jin, X. Chen, X. Mu, "A Novel Quadratic Boost Converter with Low Inductor Currents", *CPSS Transactions on Power Electronics and Applications*, Vol. 5, No. 1, 2020, pp. 1-10.
- [13] Y. M. Chen, A. Q. Huang, X. Yu, "A high step-up three-port DC-DC converter for stand-alone PV/battery power systems", *IEEE Transactions on Power Electronics*, Vol. 28, No. 11, 2013, pp. 5049-5062.

- [14] B. R. Lin, C. W. Chu, "Hybrid DC–DC Converter with High Efficiency, Wide Zvs Range, and Less Output Inductance", *International Journal of Circuit Theory and Applications*, Vol. 44, No. 5, 2016, pp. 996-1011.
- [15] N. A. Dung, P. P. Hieu, Y. C. Hsieh, J. Y. Lin, Y. C. Liu, H. J. Chiu, "A Novel Low-Loss Control Strategy For Bidirectional DC–DC Converter", *International Journal of Circuit Theory and Applications*, Vol. 45, No.11, 2017, pp. 1801-1813.
- [16] R. Faraji, H. Farzanehfard, "Soft-Switched Non-Isolated High Step-Up Three-Port Dc-Dc Converter for Hybrid Energy Systems", *IEEE Transactions on Power Electronics*, Vol. 33, No. 12, 2018, pp. 10101-10111.
- [17] J. Leyva-Ramos, M. G. Ortiz-Lopez, L. H. Diaz-Saldierna, J. A. Morales-Saldana, "Switching Regulator Using a Quadratic Boost Converter for Wide DC conversion ratios", *IET Power Electronics*, Vol. 2, No. 5, 2009, pp. 605-613.
- [18] J. A. Morales-Saldana, R. Galarza-Quirino, J. Leyva-Ramos, E. Carbajal-Gutierrez, M. G. Ortiz-Lopez, "Multiloop Controller Design for a Quadratic Boost Converter", *IET Electric Power Applications*, Vol. 1, No. 3, 2007, pp. 362-367.
- [19] J. A. Morales-Saldana, R. Loera-Palomo, E. Palacios-Hernandez, J. L. Gonzaz-Martinez, "Modelling and Control of a DC-DC Quadratic Boost Converter with R2P2", *IET Power Electronics*, Vol. 7, No. 1, 2014, pp. 11-22.
- [20] O. Lopez, L. G.Vicuna, M. Castilla, J. Matas, M. Lopez, "Sliding-Mode-Control design of a High-Power-Factor Buck-Boost Rectifier", *IEEE Transactions on Industrial Electronics*, Vol. 46, No. 3, 1999, pp. 604-612.
- [21] O. Ray, S. Mishra. "A Multi-Port Converter Topology with Simultaneous Isolated and Non-Isolated Outputs," *Proceedings of the 39th Annual Conference of the IEEE Industrial Electronics Society*, Vienna, Austria, 10-13 November 2013, pp. 7118-7123.
- [22] O. Ray, S. Mishra, "and Ac Outputs", *IEEE Transactions on Industry Applications*, Vol. 50, No. 2, 2014*, pp. 1082–1093.
- [23] S. Poshtkouhi, O. Trescases, "Multi-Input Single-Inductor Dc-Dc Converter for MPPT in Parallel-Connected Photovoltaic Applications", *Proceedings of the Twenty-Sixth Annual IEEE Applied Power Electronics Conference and Exposition*, Fort Worth, TX, USA, 2011, pp. 41-47.
- [24] M. C. Mira, Z. Zhang, A. Knott, M. A. E. Andersen, "Power Flow Control of A Dual-Input Interleaved Buck/Boost Converter With Galvanic Isolation For Renewable Energy Systems", *Proceedings of the IEEE Applied Power Electronics Conference and Exposition*, Charlotte, NC, USA, 2015, pp. 3007-3012.
- [25] H. Keyhani, H. A. Toliyat, "Single-Stage Multistring PV Inverter With an Isolated High-Frequency Link and Soft-Switching Operation", *IEEE Transactions on Power Electronics*, Vol. 29, No. 8, 2014, pp. 3919-3929.
- [26] S. S. Nag, S. K. Mishra, "A Multi-Input Single-Control (MISC) Battery Charger for Dc Nanogrids", *Proceedings of the IEEE ECCE Asia Downunder*, Melbourne, VIC, Australia, 3-6 June 2013, pp. 304-310.
- [27] F. Chen, R. Burgos, D. Boroyevich, D. Dong, "Control Loop Design of a Two-Stage Bidirectional Ac/Dc Converter for Renewable Energy Systems", *Proceedings of the IEEE Applied Power Electronics Conference and Exposition-APEC*, Fort Worth, TX, USA, 16-20 March 2014, pp. 2177-2183.
- [28] S. Poshtkouhi, M. Fard, H. Hussein, L. M. D. Santos, O. Trescases, M. Varlan, T. Lipan, "A Dual-Active-Bridge Based Bi-Directional Micro-Inverter with Integrated Short-Term Li-Ion Ultra-Capacitor Storage and Active Power Smoothing for Modular PV Systems", *Proceedings of the IEEE Applied Power Electronics Conference and Exposition-APEC*, Fort Worth, TX, USA, 16-20 March 2014, pp. 643-649.
- [29] D. Dong, F. Luo, X. Zhang, D. Boroyevich, P. Mattavelli, "Grid- Interface Bidirectional Converter For Residential DC Distribution Systems; Part 2: AC and Dc Interface Design with Passive Components Minimization", *IEEE Transactions on Power Electronics*, Vol. 28, No. 4, 2013, pp. 1667-1679.
- [30] D. Dong, I. Cvetkovic, D. Boroyevich, W. Zhang, R. Wang, and P. Mattavelli, "Grid-Interface Bidirectional Converter for Residential DC Distribution Systems; Part One: High-Density Two-Stage Topology", *IEEE Transactions on Power Electronics*, Vol. 28, No. 4, 2013, pp. 1655-1666.